

Optical Device Design With Arbitrary Output Intensity as a Function of Input Voltage

M. R. Fetterman and H. R. Fetterman, *Fellow, IEEE*

Abstract—We show that the designs for optical digital signal processing can be used to construct a device that gives an arbitrary function $I(V)$, where I is the output signal intensity and V is the input voltage. This is done by applying the same voltage V to several electrodes in the system, and does not require changing the input optical frequency. This device will have applications to modulator linearization and correction for amplifier distortion. We present a numerical simulation of the device. We study the device as a function of wavelength and voltage.

Index Terms—Electrooptic modulation, optical signal processing.

IN [1]–[5], the researchers show that, using structures similar to those found in digital signal processing (DSP), it is possible to implement optical filters. These filters can be designed for arbitrary transfer functions in phase as well as amplitude. For example, we can generate linear dispersion or a notch filter. Using the electrooptic effect, we can (theoretically) change the filter shapes at gigahertz rates. Such filters have been experimentally investigated in silicon, where thermal tuning was used to change the index of refraction. Currently, we are investigating fabrication of these devices in electrooptic polymers [6], so that much higher data rates will be accessible.

Consider an optical digital filter as described in [1]–[5]. Such a filter could have the response $f(\omega)$, as shown in Fig. 1(a), with respect to optical frequency ω . In this letter, we show that, given such a filter, we can then generate a filter with an arbitrary transfer function $f(V)$, with respect to voltage V , as shown in Fig. 1(b).

We note the related work of [7] and [8], in which the authors cascade N Mach–Zehnder modulators to generate linear signals for CATV applications, with $N = 2$. Our work represents a generalization and extension of [6], as we use several infinite impulse response (IIR) filters to obtain arbitrary response functions. Applications of this work include linearizing optical modulators and optoelectronic linearization of electronic amplifiers.

We now describe our proposed device. For DSP, it is often convenient to work in the z domain, where the relationship [9] between z and the optical frequency ω is given by

$$z^{-1} = r \exp(i\omega\tau). \quad (1)$$

The optical DSP structure [1]–[5] allows us to form a transfer function given by $S(z) = F(z)/G(z)$, where $F(z)$ and $G(z)$ are polynomial functions of z^{-1} . By tuning phase shifters on

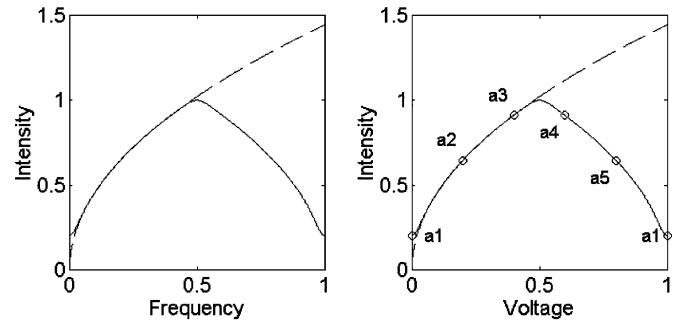


Fig. 1. For the values of the filter coefficients shown in this plot, see Table I. (a) Assume that we can construct a filter with an arbitrary transfer function $f(\omega)$ so that we may plot I , the output intensity, as a function of ω , the optical frequency. (b) As described in the text, we add signal electrodes to each filter element. Then, we can generate an arbitrary output $I(V)$ as a function of voltage, where V is a single signal voltage.

TABLE I
FILTER COEFFICIENTS FOR THE FOURTH-ORDER IIR FILTER SHOWN IN FIG. 1. FIRST ROW GIVES THE NONRECURSIVE COEFFICIENTS M , AND THE SECOND ROW GIVES THE RECURSIVE COEFFICIENTS N , SO THAT THE FILTER TRANSFER FUNCTION IS GIVEN BY $H(z) = (M_0 + M_1z^{-1} + M_2z^{-2} + M_3z^{-3} + M_4z^{-4}) / (1 + N_1z^{-1} + N_2z^{-2} + N_3z^{-3} + N_4z^{-4})$

Filter Coefficients	I	z^{-1}	z^{-2}	z^{-3}	z^{-4}
M (non-recursive)	0.63	-0.34	-0.30	0.11	0.01
N (recursive)	1.00	0.00	-0.43	0.00	0.01

the waveguides, either thermally or electrooptically, we can dynamically change $F(z)$ and $G(z)$, thereby changing $S(z)$. Since we can choose $S(z)$ and z is related to ω by (1), we can design frequency filters. The resolution of the filter function $S(z)$ will depend on the number of elements in the filter. The more elements, the higher resolution, but there will be a price in terms of optical loss and fabrication complexity.

Fig. 2 shows a design for a fourth-order coherent two-port optical delay-line circuit, after [5]. This consists of four unit elements, where each element has a ring waveguide and a symmetric Mach–Zehnder. Each element requires two directional couplers, labeled as θ_1 and θ_2 in Fig. 2, and two phase shifters, labeled as ϕ_1 and ϕ_2 . There is also one directional coupler at the beginning of the structure. The delay τ in (1), shown in the ring waveguide of Fig. 2, is determined by the physical waveguide design and will not change as voltage is applied to the control electrodes.

In this letter, we add phase electrodes (which we will refer to as signal electrodes), labeled as β in Fig. 2, to the optical DSP structures. Specifically, a signal electrode is inserted into the ring waveguide of each element. We apply the same voltage

Manuscript received November 17, 2003; revised August 8, 2004.

The authors are with the Electrical Engineering Department, University of California, Los Angeles, CA 90024 USA (e-mail: fetter@ee.ucla.edu).

Digital Object Identifier 10.1109/LPT.2004.836908

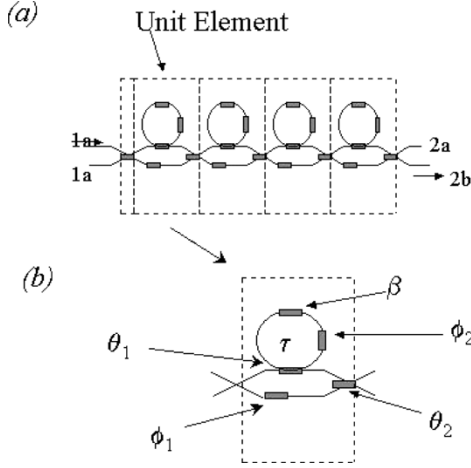


Fig. 2. This schematic, after [5], shows a fourth-order coherent two-port optical delay line circuit, where we have added signal electrodes to implement (2). (a) The fourth-order filter is implemented in four identical stages. (b) One stage contains five tunable electrodes.

V , which we refer to as the signal voltage, to all of the signal electrodes. The signal electrodes effectively modify (1) so that

$$z^{-1} = r \exp(i\omega\tau) \exp\left(\frac{i\pi V}{V_\pi}\right). \quad (2)$$

In (2), V_π is the voltage required to shift the optical phase by π . Assume that we hold the optical frequency ω constant. It follows from (2) that we can change z^{-1} as a function of voltage, rather than as a function of frequency. So, since the output intensity depends on the transfer function $S(z)$, we have designed a filter based on voltage, rather than frequency. If $S(\omega, V)$ is the filter response as a function of frequency and voltage, and $\Delta\omega = (\pi/\tau)(\Delta V/V_\pi)$, then, using (2), we find that

$$S(\omega_0 + \Delta\omega, V = 0) = S(\omega_0, V = \Delta V). \quad (3)$$

A more rigorous proof of (2) and (3) is implied in [5]. We note that this result should apply to different implementations of optical DSP [1]–[4] and not just to the design of [5], because (2) is written in a general form. The device is periodic in ω with periodicity $2\pi/\tau$, and periodic in V with period $2V_\pi$.

As compared to the original optical filter, only one additional electrode per stage is required to implement (2). A directional coupler precedes the entire structure, and there are five electrodes per stage, so that the total number of tunable elements for the fourth-order filter is 21. Typically, we may require a fast response as a function of V , and a somewhat slower response to tune the entire filter response function. Then, we may make the control electrodes $\{\theta_1, \theta_2, \phi_1, \phi_2\}$ thermoelectrically tunable, and the signal electrodes $\{\beta\}$ electrooptically tunable.

We now simulate a fourth-order filter with this design, and estimate performance parameters. In Fig. 1(a), we show the response in the wavelength domain, corresponding to the filters described in [1]–[5]. In the units of Fig. 1(a), we let $\omega = 0$ correspond to an arbitrary optical frequency ω_a and $\omega = 1$ correspond to $\omega_a + 2\pi/\tau$. As a reasonable physical value, we

could choose the length of the ring waveguide in Fig. 2 to be $L_R = 1$ cm. Then, $\tau = c/nL_R$, and the free spectral range (FSR) will be $\text{FSR} = 1/\tau = 30$ GHz, with the index of refraction $n = 1.5$ in polymer.

The dotted line in Fig. 1 represents the desired curve, which goes as $I \propto \omega^{1/2}$, and the solid curve shows the simulated filter. The values of the filter coefficients used to generate Fig. 1 are given in Table I, with the standard form described in the caption to this table. The filter is normalized as in [3] and [4], so that the maximum of the transfer function is one. We chose to match the filter to the curve until $\omega = 0.5$ (in normalized units), and then make the filter symmetrical about this point, because of the periodicity constraint of such filters.

In Fig. 1(b), the x axis is normalized so that $2V_\pi = 1$. If the electrode has length L_E , then $V_\pi L_E$ for the electrode is typically a constant, which we denote as M . For the polymer electrooptical material [6], $M = 9$ Vcm. With $L_R = 1$ cm, we would then obtain $V_\pi = 9$ V. We have labeled six points on the curve as $a1, \dots, a5, a1$, and these values will be referred to later in the letter.

The function shown in Fig. 1(b) is $I_{\text{out}} \propto V^{1/2}$, where I_{out} is the output optical intensity and V is the signal voltage. The control voltages determine the functional form $I_{\text{out}} \propto V^{1/2}$.

Next, we consider the relation between the modulation rate, the FSR, and the input laser bandwidth. The parameter τ determines the device FSR. Consider the application where we have a single optical frequency and we wish to modulate the voltage V at the highest possible data rate. The laser should have a much narrower bandwidth than the filter bandwidth so that it only samples one point of the filter. We take the laser linewidth as $\Delta\omega_0$, and we modulate the device electrodes with frequency $\Delta\omega_1$, broadening the bandwidth by $2\Delta\omega_1$. For an N th-order filter, the width of the filter's frequency variations will be approximately FSR/N , assuming that the poles and zeros are equally spaced. The condition on the FSR becomes

$$\frac{\text{FSR}}{N} > \Delta\omega_0 + 2\Delta\omega_1. \quad (4)$$

For parameters $N = 8$, $\Delta\omega_0 = 10$ MHz, $\Delta\omega_1 = 1$ GHz, the FSR should be greater than $f = 16$ GHz. The waveguide parameters we described earlier gave an FSR of 30 GHz, so these device requirements are reasonable.

To further examine this relation, we simulate the device behavior as the optical bandwidth changes. We consider the fourth-order function described in Fig. 1, with $\text{FSR} = 30$ GHz. We assume a Gaussian optical source with bandwidth 10 kHz, 5 GHz, and 10 GHz. The bandwidth could arise from a broad input source or from a higher modulation frequency. Fig. 3 shows the resultant calculation. The 10-kHz optical bandwidth waveform matches the square root curve of Fig. 1, but as the bandwidth broadens, the curves broaden and the match degrades. Also note that at the broader optical bandwidth, the filter function no longer goes to zero at the edges of the voltage range. This results from the periodicity of the filter.

There is also a relation between the driving voltage and the FSR. For the ring waveguide [10], $L_E \leq L_R$, as the electrode

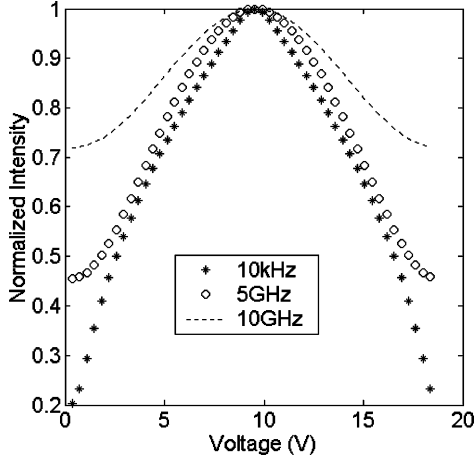


Fig. 3. Here we simulate the device response of Fig. 1. We include three different optical bandwidths of the optical source, 10 GHz, 5 GHz, and 10 kHz. The narrow 10-kHz source faithfully reproduces the desired curve. As the source optical bandwidth broadens, the resultant curve also broadens.

cannot be longer than the ring waveguide on which it is fabricated, and it follows that:

$$V\pi \geq \text{FSR} \left(\frac{n_{\text{eff}}M}{c} \right). \quad (5)$$

So, as we make IIR filters with a wider FSR by using shorter ring waveguides, the $V\pi$ will increase. Also, from (4) and (5) we can conclude that higher modulation frequencies require a higher $V\pi$. The issues raised by (4) and (5) will generally apply to electrooptical IIR structures, as electrooptical modulators typically have less index change than thermo-optical modulators. Designing an IIR structure with a low $V\pi$ and a high modulation frequency would be a subject for further research.

The functionality of this device is accomplished without changing the input optical frequency. Above, we considered the effects of broadening the optical frequency. We may also design our filter to operate as a function of voltage and optical frequency. In Fig. 4, the y axis represents ω , normalized from zero to one as in Fig. 1(a), and the x axis represents V , normalized as in Fig. 1(b), and we use these normalized units when referring to Fig. 4. On the voltage-wavelength axes of Fig. 4, we then plot the same function as illustrated in Fig. 1, using the values a_1, \dots, a_5, a_1 from Fig. 1. With (2), we can find the response of the device as a function of voltage and wavelength. The values along the optical frequency axis of Fig. 4, with $V = 0$, correspond to the filter of Fig. 1(a), and the values along the voltage axis, with $\omega = 0$, correspond to the filter of Fig. 1(b).

With some restrictions, we can also make a filter as a function of wavelength and voltage, which could be useful in a dense wavelength-division-multiplexing application. We limit V to

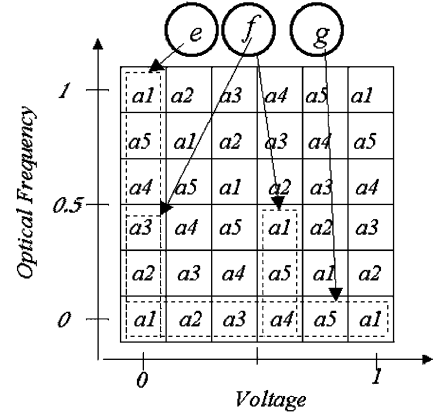


Fig. 4. Device response as a function of optical frequency and voltage. The variables a_1, \dots, a_5 correspond to the values of the filter function from Fig. 1(b). The values along the optical frequency axis, outlined by a dotted box labeled e , correspond to Fig. 1(a), which is a filter as a function of wavelength. The values along the voltage axis, outlined by the dotted box labeled g , correspond to Fig. 1(b), which is the filter as a function of voltage. We can also make a filter with the two voltages $V = 0$ and $V = 0.6$, and the optical frequencies from $\omega = 0$ to $\omega = 0.5$. These values are enclosed in two dotted boxes, labeled f .

the two discrete values 0 and 0.6, and we limit ω from 0 to 0.5. Then, we obtain different filter functions, as a function of wavelength, at these two voltages. One constraint is that the filter will have the same value at the start of the frequency range as at the end of the frequency range.

REFERENCES

- [1] C. K. Madsen, "General IIR optical filter design for WDM applications using all-pass filters," *J. Lightw. Technol.*, vol. 18, no. 6, pp. 860–868, Jun. 2000.
- [2] C. K. Madsen and J. H. Zhao, *Optical Filter Design and Analysis*. New York: Wiley, 1999.
- [3] K. Jinguji and M. Oguma, "Synthesis of coherent two-port lattice-form optical delay circuits," *J. Lightw. Technol.*, vol. 13, no. 1, pp. 73–82, Jan. 1995.
- [4] —, "Optical half-band filters," *J. Lightw. Technol.*, vol. 18, no. 2, pp. 252–259, Feb. 2000.
- [5] K. Jinguji, N. Takato, Y. Hida, T. Kitoh, and M. Kawachi, "Two-port optical wavelength circuits composed of cascaded Mach–Zehnder interferometers with point-symmetrical configurations," *J. Lightw. Technol.*, vol. 14, no. 10, pp. 2301–2310, Oct. 1996.
- [6] D. H. Chang, H. R. Fetterman, H. Erlig, H. Zhang, M.-C. Oh, C. Zhang, and W. H. Steier, "39-GHz optoelectronic oscillator using broad-band polymer electrooptic modulator," *IEEE Photon. Technol. Lett.*, vol. 14, no. 2, pp. 191–193, Feb. 2002.
- [7] H. Skeie and R. V. Johnson, "Linearization of electrooptic modulators by a cascade coupling of phase modulating electrodes," *Proc. SPIE*, vol. 1583, pp. 153–164, 1991.
- [8] H. Skeie, "An optically linearized modulator for CATV applications," *Proc. SPIE*, vol. 2291, pp. 237–238, 1994.
- [9] P. Lynn and W. Fuerst, *Introductory Digital Signal Processing With Computer Applications*. New York: Wiley, 1998.
- [10] P. Rabiei, W. H. Steier, C. Zhang, C. Wang, and H.-J. Lee, "Polymer micro-ring modulator with 1 THz," in *CLEO 2002 Tech. Dig.*, vol. 2, Paper CDB8-1.